Journal of Solid State Chemistry 182 (2009) 622–629

Contents lists available at ScienceDirect

Journal of Solid State Chemistry

journal homepage: www.elsevier.com/locate/jssc

IM-16: A new microporous germanosilicate with a novel framework topology containing *d4r* and *mtw* composite building units

Yannick Lorgouilloux [a], Mathias Dodin [a], Jean-Louis Paillaud [a,*], Philippe Caullet [a], Laure Michelin [a], Ludovic Josien [a], Ovidiu Ersen [b], Nicolas Bats [c]

[a] *Laboratoire de Matériaux à Porosité Contrôlée (UMR 7016 CNRS, ENSCMu, UHA), 3 rue Alfred Werner, 68093 Mulhouse Cedex, France*
[b] *IPCMS-GSI, UMR 7504 (CNRS, ULP), 23 rue du Loess, BP 43, 67034 Strasbourg, Cedex 2, France*
[c] *IFP-Lyon, BP3, 69360 Solaize, France*

ARTICLE INFO

Article history:
Received 8 October 2008
Received in revised form
1 December 2008
Accepted 15 December 2008
Available online 24 December 2008

Keywords:
Zeolite
IM-16
Hydrothermal synthesis
Ionic liquid
3-Ethyl-1-methyl-3*H*-imidazol-1-ium
Structure from powder XRD data
Rietveld refinement
Framework topology
Composite building units

ABSTRACT

The synthesis and the structure of IM-16 a new germanosilicate with a novel zeolitic topology prepared hydrothermally with the ionic liquid 3-ethyl-1-methyl-3*H*-imidazol-1-ium as the organic structure-directing agent are reported. The structure of calcined and partially rehydrated IM-16 of chemical formula $|(H_2O)_{0.16}|[Si_{3.47}Ge_{2.53}O_{12}]$ was solved from powder XRD data in space group *Cmcm* with $a = 15.0861(2)$ Å, $b = 17.7719(3)$ Å, $c = 19.9764(3)$ Å, $V = 5355.84(12)$ Å^3 ($Z = 16$). This new zeolite framework type contains 10-MRs channels and may be described from the *d4r* and *mtw* composite building units.

1. Introduction

The search for new materials is crucial for the industry. In particular, porous materials with unusual catalytic or adsorption properties have drawn the industrial partners' attention to basic researches on microporous materials such as zeolites with new framework topologies. Thus, after the pioneering work of Barrer and Milton in the 1940s, several synthetic strategies have emerged [1]. Among them, the use of OH^- or F^- (fluoride route) as mineralizers in combination with the development of new organic structure directing agents (OSDAs) and the modification of the concentration of the precursor gels allowed the synthesis of many novel zeolites, most of them having no natural counterparts [2]. Another important approach consisted in the partial or total substitution of the classical silicon and aluminum atoms by heteroelements such as phosphorus [3], titanium, zinc, gallium, boron, or germanium [4]. The latter was the most recently introduced in the hydrothermal synthesis of microporous materials and its use was very successful. The main reason lies in the fact that, whereas germanium is the closest analogue to silicon and presents some properties analogous to it, it has the benefit over silicon that in addition to tetrahedra (Td), it can also be found in 5- (square pyramidal (Sp) or trigonal bipyramidal (Tbp)) and 6- (octahedral (Oh)) coordination spheres [5]. As a result, porous germanates for which the framework consists exclusively of Td (as in e.g. ASU-7 (**ASV**) [6], FOS-5 (**BEC**) [7], IM-10 (**UOZ**) [8] or IM-12 (**UTL**)) [9], or of a combination of different types of polyhedra have been synthesised during the last decade [5,10]. It should be noted that many of these new germanium-based zeolites contain *d4r* (double 4-membered rings) composite building units (CBUs) [11].

In addition to the hydrothermal syntheses in presence of heteroelements such as those just mentioned above, non-aqueous solvents were also engaged with success in the preparation of zeolites [1]. It appears from these studies that the viscosity of the non-aqueous solvents is a key factor for the crystallisation of the zeolites and, depending on its value, it makes the synthesis of large crystals possible. Since 2004, a novel type of solvothermal synthesis of zeolites named the ionothermal route has been developed [12]. Here, ionic liquids such as imidazolium and pyrrolidinium derivatives or deep eutectic mixtures are used as both the solvent and the OSDA. However, up to now, this method led to the formation of new phosphate-based microporous

* Corresponding author. Fax: +33 3 89 33 68 85.
E-mail address: Jean-Louis.Paillaud@uha.fr (J.-L. Paillaud).

0022-4596/$ - see front matter © 2009 Elsevier Inc. All rights reserved.
doi:10.1016/j.jssc.2008.12.002

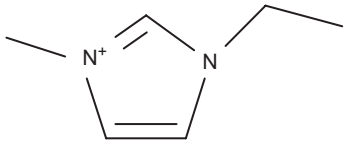

Fig. 1. 3-Ethyl-1-methyl-3*H*-imidazol-1-ium.

materials and organic–inorganic porous hybrid compounds but no silica-based porous material [13]. Besides, the ionic liquids themselves can act as classical OSDAs in aqueous media. Indeed, by using the fluoride route Zones et al. [2b] synthesised pure silica zeolites of **TON**, **ITW** and **MTT** topologies using the OSDAs 1,3-dimethyl-3*H*-imidazol-1-ium, 1,2,3-trimethyl-3*H*-imidazol-1-ium and 1,3-diisopropyl-3*H*-imidazol-1-ium, respectively [2b]. Interestingly these OSDAs are very selective regardless of the molecular ratio H_2O/SiO_2 of the starting synthesis gel. Herein, we report on the synthesis and characterisation of a new microporous germanosilicate having a novel framework topology prepared with the ionic liquid 3-ethyl-1-methyl-3*H*-imidazol-1-ium (Fig. 1) as the OSDA, namely IM-16 [14].

2. Experimental

2.1. Synthesis

The reactants used to prepare IM-16 were TEOS (>98% Fluka), Aerosil 200 (>98% Degussa), amorphous germanium oxide GeO_2 (>99.99%, Aldrich), HF acid (40%, Carlo Erba), distilled water, and 3-ethyl-1-methyl-3*H*-imidazol-1-ium bromide (98%, Solvionic), which was transformed into its OH form by ion exchange in water (Dowex SBR LC NG, OH Form (Supelco)). The OSDA solutions were concentrated by lyophilisation when necessary. The chemical compositions of the starting gels are listed in Table 1. All the syntheses were performed in 2 mL Teflon-lined autoclaves at 170 °C for 14 days.

2.2. Scanning electron microscopy

The morphologies and sizes of the crystals were determined by scanning electron microscopy (SEM) using a Philips XL30 FEG SEM.

2.3. ^{19}F MAS NMR spectroscopy

The ^{19}F MAS NMR experiment was performed on a Bruker DSX 400 spectrometre (frequency 376.5 MHz, pulse width 4 μs, flip angle $\pi/2$, recycling time 40 s, spinning rate 25 kHz, chemical shift standard $CFCl_3$).

2.4. X-ray analysis

The PXRD of calcined IM-16 samples were collected on a PANalytical MPD X'Pert Pro diffractometre in a Debye–Scherrer geometry equipped with a capillary sample holder, a hybrid mirror monochromator ($\lambda = 1.5406$ Å) which gives the monochromatic parallel beam geometry and an X'Celerator real-time multiple strip detector (active length = 2.122°(2θ)). Quickly after calcination (540 °C under air), the grinded powder of IM-16 was introduced in the Mark-tube made of special glass (no. 14, outside diametre 0.3 mm, Hilgenberg Gmbh) then the capillary tube was sealed and mounted on a precise goniometric head which is screwed on a rotary sample stage, the spinning rate was 1 rotation per second. The powder pattern was collected at 295 K in the range $6.5 < °2\theta < 80$, step = 0.008°2θ, time/step = 3350 s, the total collecting time was about 64 h. The step size has been interpolated to 0.02 for the Rietveld refinement. The PXRD pattern of calcined IM-16 was indexed with a C-centred orthorhombic unit cell parameters, $a = 15.0820(14)$ Å, $b = 17.7713(21)$ Å, $c = 19.983(3)$ Å and $V = 5355.9(15)$ Å^3 (after refinement) by the Louër's DICVOL91 [15] indexing routine of the STOE WinXPow program package [16]. The observed systematic extinctions suggested *C*222$_1$, *C*222, *Cmm*2, *Cmcm* and *Cmmm* as possible space groups but the general reflection condition (*h0l*: $h, l = 2n$) of space group *Cmcm* (#63) improves slightly the refinement and gives the highest figure of merit value ($F(30) = 111.7$). For the structure determination the extracted intensities of the reflections up to 60°(2θ) (1.540 Å) were taken; whereas for the Rietveld refinement the complete pattern was used. The structure of calcined IM-16 was solved by the direct methods in space group *Cmcm* using the EXPO2004 software [17], an ensemble of structure determination programs. The Rietveld refinement was performed using the GSAS package [18].

The atomic coordinates of the framework atoms (i.e. *T* and O atoms with *T*=Si or Ge) proposed by the direct methods and minimised by molecular modelling [19] were used as the starting model. All the atoms were refined isotropically. Soft restraints were placed on the bond lengths and angles of the framework (*T*–O = 1.68(10) Å and O–*T*–O = 109.5(30)°). For the Rietveld refinement, on each *T* atom site, a silicon atom and a germanium atom were both placed at the same position with the sum of their occupancy factors constrained to be 1. After refinement of the framework, successive calculated Fourier difference maps revealed two scattering densities inside the void volume attributed to the presence of adsorbed water molecules. Then, two oxygen atoms have been placed on these positions and refined (positions and occupancy factors). Further details on crystallographic and Rietveld refinement data are given in Table 2. The final atomic parameters are listed in Table 3. In Tables 4 and 5 bond distances and selected bond angles are reported, respectively. A CIF file is also available as supplementary data. The final plot of the Rietveld refinement is given in Fig. 2.

Table 1
Selection of the most representative synthesis of zeolite IM-16 with 3-ethyl-1-methyl-3*H*-imidazol-1-ium as OSDA.

Sample	Molar gel composition (T = Si+Ge)				Material
	H_2O/T	R/T	HF/T	Si/Ge	
1[a]	20	0.5	0	0.6:0.4	**TON**+**MFI**+Arg[c]
2[a]	20	1	0	0.6:0.4	**MFI**+ε?[d]
3[a]	8	0.5	0.5	1:0	Amorphous
4[a]	8	0.5	0.5	0.8:0.2	IM−16+ε?[d]
5[a]	8	0.5	0.5	0.6:0.4	IM−16+ε?[d]
6[a]	8	0.5	0.5	0.4:0.6	*Q*[c]+IM−16
7[a]	8	0.5	0.5	0.2:0.8	*Q*[c]
8[a]	8	0.6	0.4	0.8:0.2	IM−16+ε?[d]
9[a]	20	1	0.5	0.6:0.4	IM−16+ε?[d]
10[a]	3	0.3	0.3	0.8:0.2	IM−16+ε?[d]
11[a]	20	1	1	0.8:0.2	IM−16+ε?[d]
12[a]	20	1	1	0.6:0.4	IM−16+ε?[d]
13[a]	20	1	1	0.5:0.5	IM−16+*Q*[e]
14[b]	20	1	1	0.8:0.2	IM−16+**MFI**
15[b]	20	1	1	0.6:0.4	IM−16+ε?[d]
16[b]	20	1	1	0.5:0.5	IM−16

Silica sources:
[a] TEOS (tetraethylorthosilicate).
[b] Aerosil 200.
[c] Argutite.
[d] ε?: small quantity of one or more unknown impurities.
[e] Quartz.

Table 2
Crystal and Rietveld refinement data of calcined and partially rehydrated IM-16.

Chemical name	IM−16
Chemical formula (asymmetric unit)	$\|(H_2O)_{0.159}\|[Si_{3.47}Ge_{2.53}O_{12}]$[a]
Space group	*Cmcm* (no. 63)
a (Å)	15.0861(2)
b (Å)	17.7719(3)
c (Å)	19.9764(3)
V (Å^3)	5355.84(12)
Z	16
Number of data points (step (°2θ))	3702 (0.02)
Number of contributing reflections	961
Number of structural parameters	182
Number of profile parameters	16
Total number of restraints (bonds, angles)	127 (55, 72)
Total number of constraints	39
[b]$R_p = \Sigma\{\|y_o-y_c\| \times \|y_o-y_b\|/y_o\|/\Sigma\|y_o-y_b\|\}$	0.0643
[b]$wR_p = \{\Sigma[w \times (y_o-y_c) \times (y_o-y_b)/y_o]^2/\Sigma[w \times (y_o-y_b)^2]\}^{1/2}$	0.0804
[c]R_{exp}	0.0378
[c]R_F	0.0584
[c]R_F^2	0.0912
[c]χ^2	4.514
Largest diff. peak and hole (e Å^{-3})	0.669, −0.609

[a] After the Rietveld refinement, the total number of extra framework oxygen atoms (Ow1 and Ow2) is about 3.385 (see Table 3) per unit cell (0.212 per asymmetric unit). However, the refinement did not take into account the scattering power of the hydrogen atoms of each water molecule. Consequently, the true number of water molecules is about 25% lower than the total number of extra framework oxygen atoms refined, i.e. about 0.159 water molecules per asymmetric unit as reported in the chemical formula of the table.

[b] y_o, y_c, y_b are y observed, y calculated and y background, respectively.

[c] The definition of these residual values are given in Ref. [18].

Table 3
Atomic coordinates, site occupancies factors and equivalent isotropic displacement parameters (Å^2) for IM-16.

Name	*X*	*Y*	*Z*	*U* [Å^2] × 100	S.O.F.
Ge1/Si1	0.3979(4)	0.38872(29)	0.44864(31)	4.15(8)	0.625(9)/0.375(9)
Ge2/Si2	0.3964(4)	0.33933(32)	0.60215(33)	4.15(8)	0.526(11)/0.474(11)
Ge3/Si3	0.1034(4)	0.28321(31)	0.59519(34)	4.15(8)	0.555(11)/0.445(11)
Si4/Ge4	0.3975(4)	0.16704(29)	0.55945(36)	4.15(8)	0.478(10)/0.522(10)
Si5/Ge5	0.2258(5)	0.39011(41)	0.67049(31)	4.15(8)	0.893(8)/0.107(8)
Si6/Ge6	0.2760(5)	0.02889(38)	0.57462(31)	4.15(8)	0.808(8)/0.192(8)
O1	0.3583(9)	0.3685(8)	0.5266(5)	4.98(26)	1
O2	0.5	0.4205(10)	0.4530(10)	4.98(26)	1
O3	0.3960(11)	0.2466(6)	0.6039(6)	4.98(26)	1
O4	0.3319(8)	0.3749(7)	0.6602(6)	4.98(26)	1
O5	0.5	0.3727(11)	0.6132(10)	4.98(26)	1
O6	0.1735(8)	0.3141(7)	0.6494(7)	4.98(26)	1
O7	0.3720(8)	0.1816(7)	0.4792(5)	4.98(26)	1
O8	0.3956(10)	0.3113(6)	0.4035(7)	4.98(26)	1
O9	0.2065(12)	0.4087(10)	0.75	4.98(26)	1
O10	0	0.3147(10)	0.6149(10)	4.98(26)	1
O11	0.3270(8)	0.1075(6)	0.5911(6)	4.98(26)	1
O12	0.5	0.1295(10)	0.5624(10)	4.98(26)	1
O13	0.3333(7)	0.4566(7)	0.4163(7)	4.98(26)	1
O14	0.1908(8)	0.4626(7)	0.6260(6)	4.98(26)	1
O15	0.2988(12)	0	0.5	4.98(26)	1
Ow1	0	-0.0082(21)	0.1602(21)	12.50	0.109(27)
Ow2	0.2488(10)	0.2285(13)	0.5504(14)	12.50	0.157(17)

2.5. TGA and DTA measurements

Thermogravimetric and differential thermal analyses (TGA, DTA) were performed under air on a Setaram Labsys thermoanalyser with a heating rate of 5 °C min^{-1} up to 1100 °C.

Table 4
Selected bond lengths (Å) in the germanosilicate IM-16, standard deviations in brackets.

Ge1/Si1	O2	1.643(9)	Si4/Ge4	O11	1.628(13)
	O8	1.645(13)		O3	1.669(13)
	O13	1.680(13)		O7	1.670(13)
	O1	1.706(12)		O12	1.685(9)
Ge2/Si2	O4	1.641(14)	Si5/Ge5	O6	1.620(14)
	O3	1.648(12)		O4	1.636(14)
	O5	1.686(9)		O9	1.648(8)
	O1	1.696(13)		O14	1.652(14)
Ge3/Si3	O6	1.610(14)	Si6/Ge6	O15	1.614(7)
	O7	1.654(12)		O11	1.628(13)
	O8	1.680(12)		O14	1.641(14)
	O10	1.703(10)		O13	1.679(13)

Table 5
Selected bond angles (°) in the silicogermanate IM-16, standard deviations in brackets.

Ge1/Si1	O2	O8	109.65(56)	Si5/Ge5	O6	O4	107.83(74)
	O2	O13	108.51(49)		O6	O9	109.38(61)
	O2	O1	110.63(56)		O6	O14	110.78(74)
	O8	O13	112.18(66)		O4	O9	109.09(57)
	O8	O1	108.46(70)		O4	O14	111.95(73)
	O13	O1	107.40(69)		O9	O14	107.79(55)
Ge2/Si2	O4	O3	111.60(69)	Si6/Ge6	O15	O11	111.04(56)
	O4	O5	108.77(54)		O15	O14	106.51(55)
	O4	O1	108.07(66)		O15	O13	110.98(59)
	O3	O5	110.63(57)		O11	O14	110.20(71)
	O3	O1	108.86(70)		O11	O13	108.09(71)
	O5	O1	108.85(55)		O14	O13	110.03(72)
Ge3/Si3	O6	O7	109.14(72)	O1	Ge2	Ge1	139.28(71)
	O6	O8	108.94(70)	O2	Ge1	Ge1	139.29(30)
	O6	O10	109.51(55)	O3	Ge2	Si4	146.67(76)
	O7	O8	112.95(68)	O4	Si5	Ge2	137.11(85)
	O7	O10	106.79(53)	O5	Ge2	Ge2	135.92(29)
	O8	O10	109.46(55)	O6	Ge3	Si5	141.18(90)
				O7	Ge3	Si4	150.44(76)
Si4/Ge4	O11	O3	109.62(63)	O8	Ge1	Ge3	145.83(76)
	O11	O7	108.83(69)	O9	Si5	Si5	148.00(30)
	O11	O12	109.20(54)	O10	Ge3	Ge3	132.63(29)
	O3	O7	112.09(69)	O11	Si4	Si6	141.00(80)
	O3	O12	109.24(56)	O12	Si4	Si4	133.17(29)
	O7	O12	107.81(54)	O13	Si6	Ge1	129.68(75)
				O14	Si6	Si5	143.04(87)
				O15	Si6	Si6	155.39(32)

2.6. ^{1}H liquid NMR spectroscopy

The exact amount of occluded OSDA molecules was determined from quantitative ^{1}H liquid NMR spectroscopy. For that, a known amount of the as-synthesised IM-16 (50 mg) was dissolved into 2 mL of HF (40% in water). Thereafter, 150 μL of a 0.282 M 1,4-dioxane/D_2O solution were added as an internal standard to the dissolved material. After homogenisation, 0.5 mL of the liquid was transferred with an equivalent volume of pure D_2O in a Teflon® tube for the NMR analysis. The spectra were recorded on a Bruker AC 400 spectrometre (not shown). The recording conditions were: frequency = 400.17 MHz; recycle time = 1 s; pulse width = 2.1 μs; pulse angle = $\pi/6$, ^{1}H chemical shifts being referenced to TMS. Thus, the ^{1}H liquid NMR spectrum gives about 9% of OSDA in as-synthesised IM-16 (sample **16**) (this percentage fluctuates from 9% to 11% for other samples).

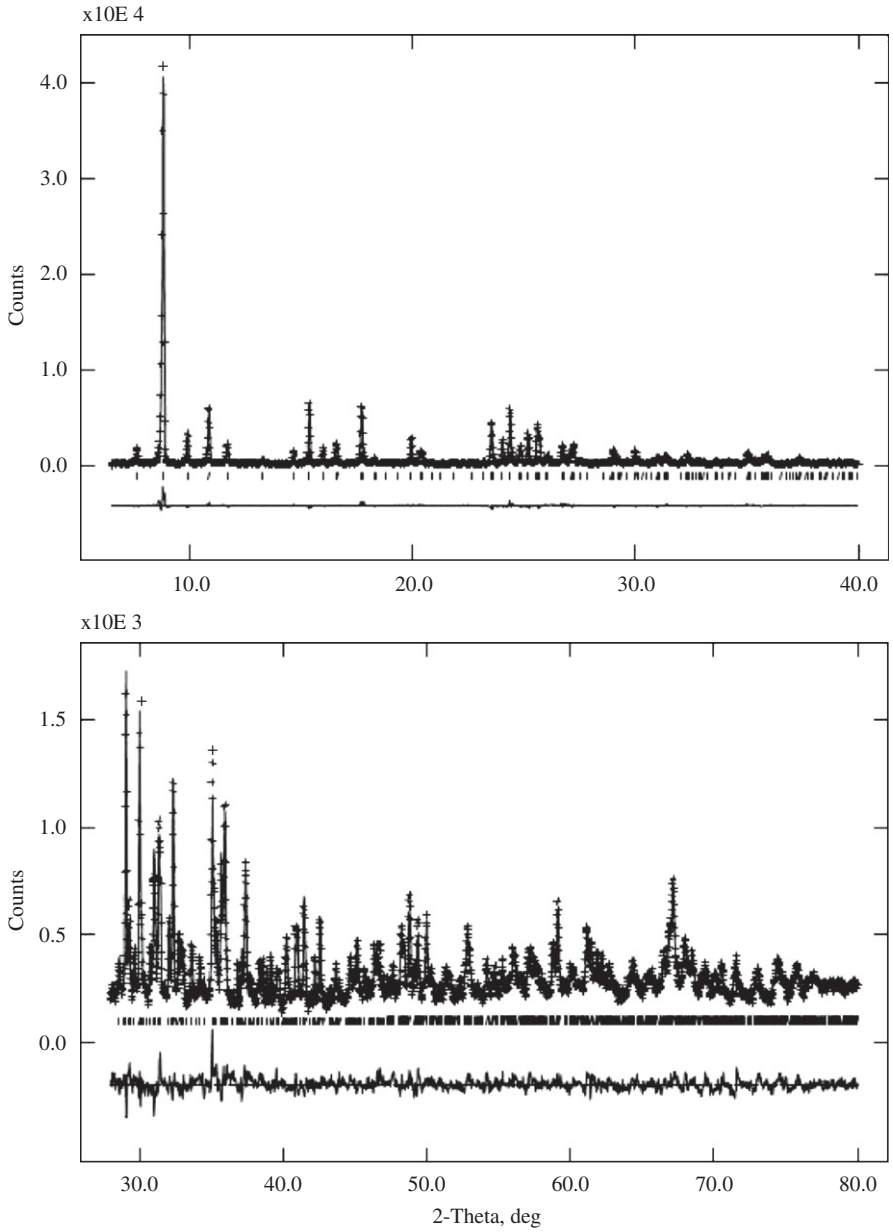

Fig. 2. Rietveld plots of calcined IM-16 (top: low angles part, bottom: high angles part) (sample **16**), experimental (+) and calculated (solid line) XRD patterns. Vertical ticks are the positions of the theoretical reflections for space group *Cmcm*. The lowest trace is the difference plot.

2.7. N_2 adsorption isotherm measurement

The microporous volume and the specific surface area of IM-16 (sample **16**) were determined from nitrogen adsorption isotherms at 77 K on a Micromeritics ASAP 2010 porosimetre using the BET method [20]. After calcination (540 °C under air) the sample was placed in a glass measurement cell that was quickly closed to avoid contact with moisture as for the X-ray data collection. Then it was degased at 350 °C under vacuum prior to the measurement.

3. Results and discussion

It appears from the various syntheses made to optimize the preparation of IM-16 that (i) the synthesis is only possible in fluorinated media and (ii) as it was observed by Zones et al. [2b], with imidazolium derivatives, its synthesis is independent of the dilution (see Table 1). The best results were obtained with Aerosil 200 as the silica source and the highest R/T molecular ratios for which almost pure or pure IM-16 are crystallised (samples **15** and **16**). Curiously, a Si/Ge molar ratio of one gives an impurity free sample despite the chemical analysis of the product (see below). Undeniably, the nature of the polysilicate species formed during the hydrolysis of TEOS should play an important role on the formation of the impurities.

The plate-like crystals of IM-16 (sample **16**), of which the sizes vary between around 1 and 20 μm, display a prismatic shape reminding the one of **MFI**-type zeolites (Fig. 3). According to the powder X-ray diffraction pattern (PXRD), sample **16** is a pure phase (see the Rietveld plot in Fig. 2). It is important to note that after a week, we decided to verify the crystallinity of the calcined sample by collecting new data using the same capillary.

The resulting PXRD pattern was typical of a partially collapsed structure which results from the presence of a small quantity of water responsible for the germanium sites hydrolysis in spite of the taken precautions. The bulk chemical analysis performed on sample **16** by AAS led to a mean Si/Ge atomic ratio of about 1.37 (see the supplementary data). However, a large heterogeneity was revealed by electron micro- and nano-probe analyses (see the supplementary data). Indeed, the measured Si/Ge molar ratio differs not only from one crystal to another but also within the crystals themselves, its value ranging from 0.95 to 2.1, a similar phenomenon being also observed for the fluoride ions.

According to the quantitative ^{1}H liquid NMR study, chemical analysis, structure determination and TG analysis (Fig. 4), the ideal chemical compositions of IM-16 are $|(C_6N_2H_{11})_{0.43}|[Si_{3.47}Ge_{2.53}O_{12}F_{0.43}]$ for the as-synthesised material and $|(H_2O)_{0.16}|[Si_{3.47}Ge_{2.53}O_{12}]$ after calcination and partial rehydration. The ^{19}F MAS NMR spectrum (Fig. 5) performed on the as-synthesised IM-16 zeolite indicates the presence of compensating F^- species occluded inside *d4r* CBUs. The asymmetric signal observed at about −10.6 ppm suggests a statistical distribution of the silicon and germanium atoms at the vertices of the *d4r* units; this point is also confirmed by the present structural study.

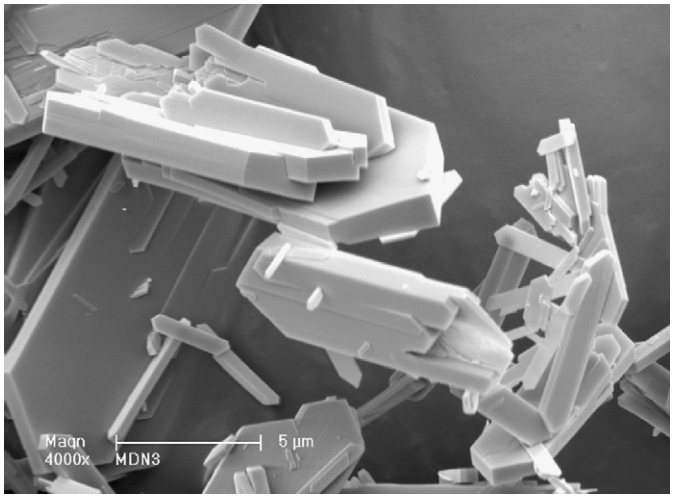

Fig. 3. SEM micrograph of IM-16 (sample **16**).

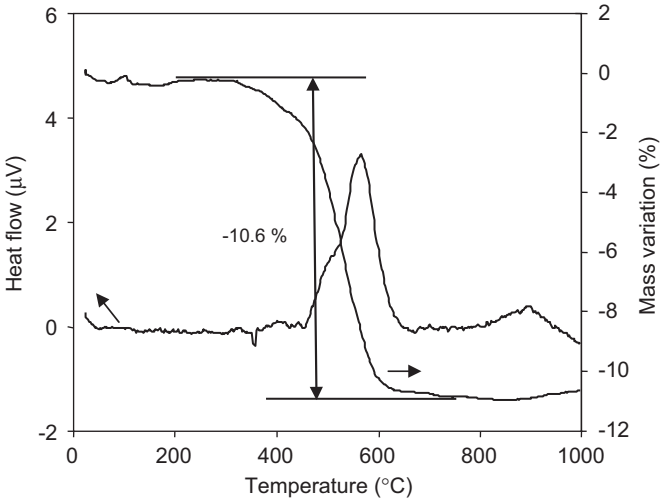

Fig. 4. TGA and DTA curves of IM-16 (sample **16**).

The structure of IM-16 contains 96 tetrahedral (*T*) atoms per unit cell and six unique crystallographic *T* sites in the asymmetric unit (Fig. 6). The statistical distribution of the silicon and germanium atoms on the *T* sites obtained at the end of the Rietveld refinement converged on a Si/Ge molar ratio of about 1.37, a value equivalent to that of the mean bulk chemical analysis (AAS). The refined total amount of adsorbed water molecules converged to about 2.54 molecules per unit cell (see footnote of Table 2). One of these adsorbed molecules (Ow2) interacts strongly with the framework and bridges *T*3 and *T*4 (Fig. 6), the *T*–O distances being 2.56(2) and 2.50(2) Å, respectively.

The framework structure of IM-16 may be described from the *d4r* and *mtw* CBUs as follow. Along the crystallographic *a*-axis, columns are formed by a stacking of *d4r* and *mtw* cages with the

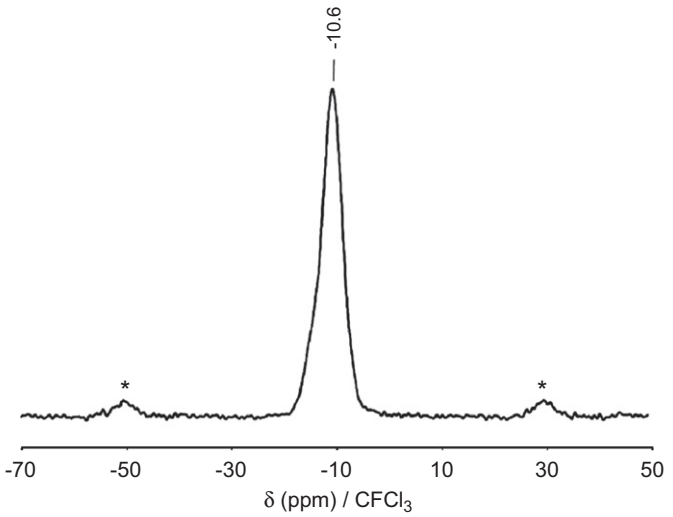

Fig. 5. ^{19}F MAS NMR spectrum of IM-16 (sample **16**). The spinning bands are marked with ∗.

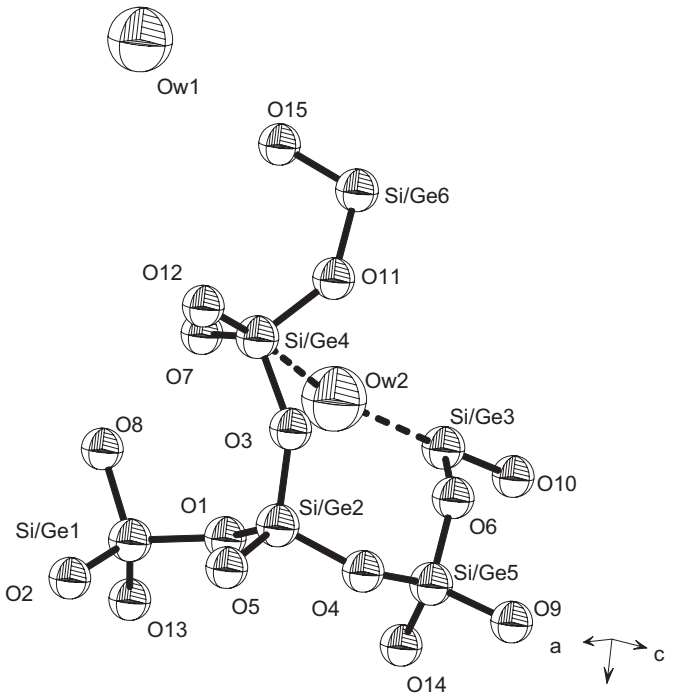

Fig. 6. ORTEP plot of the asymmetric unit of calcined IM-16.

sequence…*d4r*-*mtw*-*d4r*-*mtw*…. These columns are connected via edges, each column being rotated by an angle of 180° compared to its immediate neighbours, the twofold axis coinciding with the bridging oxygen O15 along *a*-axis (Figs. 7a and b). Thus, in the *a*,*b*-plane, *mtw*,*d4r*-layers are formed (Fig. 7c). Then, along *c*-axis, these layers are connected via bridging oxygen atoms O9 to form IM-16 (Fig. 7d). Note that each *mtw*,*d4r*-layers is a mirror image of its immediate neighbours (Fig. 7d). Thus the three-dimensional

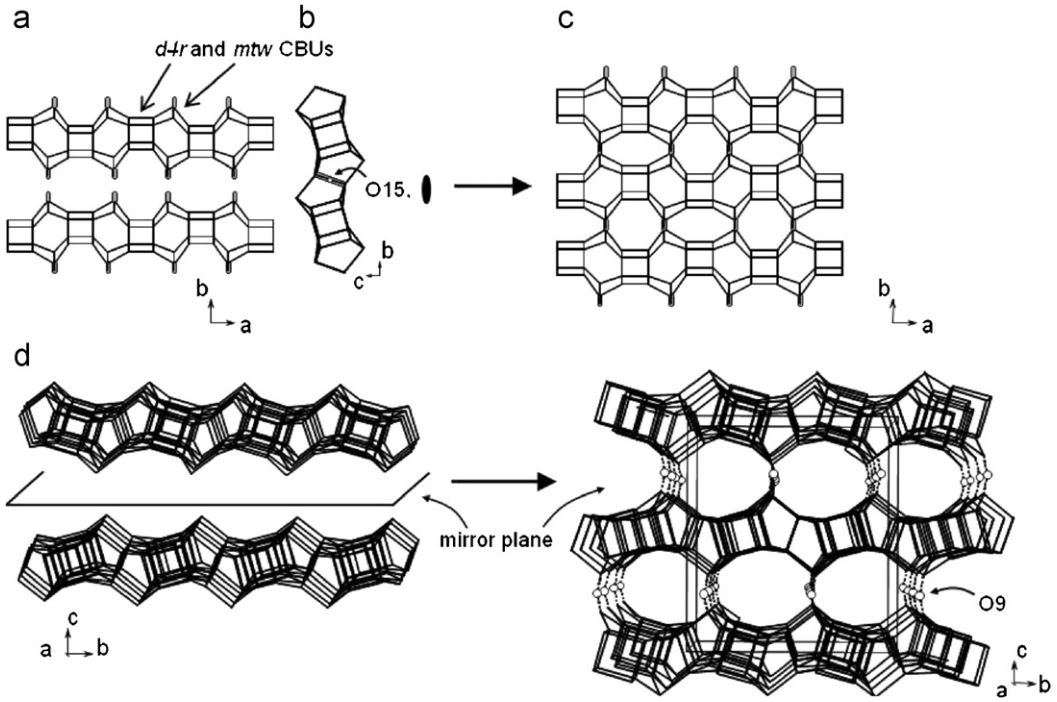

Fig. 7. Stacking modes for IM-16: (a) two *d4r*,*mtw*-columns (*a*,*b*-plane), one being rotated by 180° compared to the other, (b) perpendicular view after connection showing the twofold-axis located on the crystallographic site O15, (c) resulting *d4r*,*mtw*-layer in the (*a*,*b*-plane) and (d) view along [100] between the layers, the mirror plane merges with the plane formed by the oxygen atoms O9. The grey bonds in bold are the sharing edges and the dashed bonds connect the layers. Excepted for O9 and O15, the oxygen atoms have been omitted for clarity.

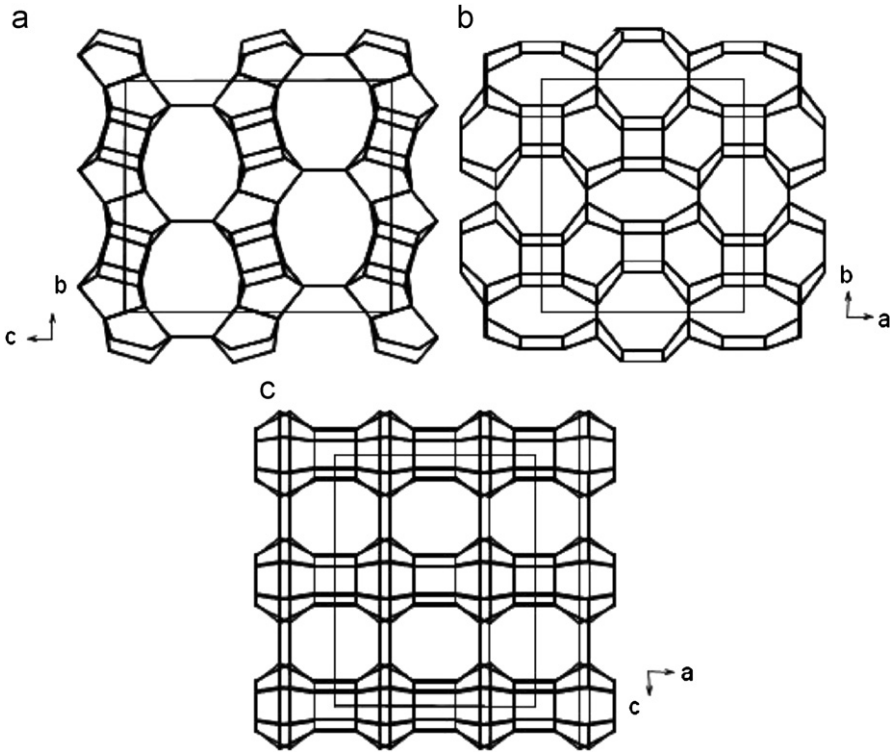

Fig. 8. Projections of the IM-16 structure along (a) [100], (b) [001] and (c) [010]. The oxygen atoms have been omitted for clarity.

Table 6
Coordination sequences and vertex symbols calculated for the framework topology of IM-16 [21].

T-atom site	N_1 to N_{12}												Vertex symbol
$T_{1,4}$ (16,1)	4	9	18	34	60	87	107	132	181	238	276	313	$4\cdot5\cdot4\cdot6\cdot4\cdot8_2$
$T_{2,3}$ (16,1)	4	9	18	36	60	84	106	135	181	235	278	318	$4\cdot5\cdot4\cdot6\cdot4\cdot8_2$
T_5 (16,1)	4	12	25	37	51	79	117	152	182	220	275	337	$5\cdot8\cdot5\cdot8\cdot6\cdot10_4$
T_6 (16,1)	4	12	21	33	54	83	116	151	181	220	275	331	$5\cdot8\cdot5\cdot8\cdot5_2\cdot6$

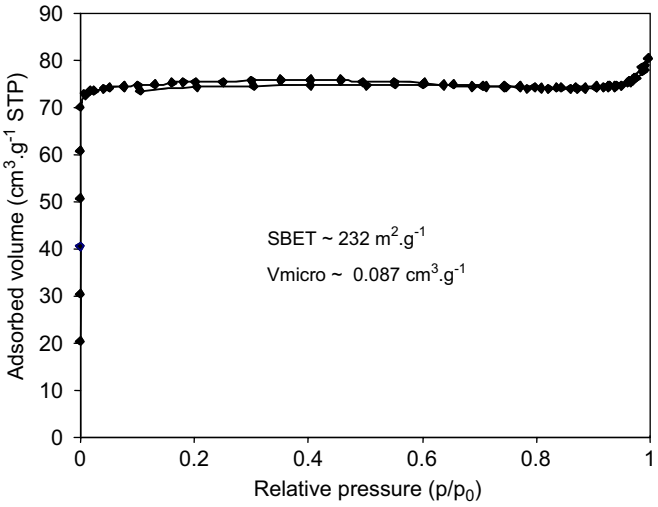

Fig. 9. N_2 adsorption–desorption isotherms of calcined IM-16 (sample **16**).

pore system of IM-16 is constituted of 10-ring pores along [100] that intersect 8-ring pores along [010] and [001] (Fig. 8), respectively. From the six crystallographic independent *T* sites of IM-16, four unique coordination sequences are calculated from TOTOPOL [21], a program computing bond geometries and topological properties for zeolite structures. These sequences are listed in Table 6 together with the vertex symbols. The N_2 adsorption isotherm of IM-16 is characteristic of a microporous material and is of type Ia following the IUPAC nomenclature (Fig. 9). The corresponding Brunauer–Emmett–Teller surface area of $232\,m^2/g^{-1}$ which is obviously underestimated for small pore microporous materials, and the microporous volume of $0.087\,cm^3/g^{-1}$ are comparable to those of small-pore zeolites. Such low values of the microporous volume and surface area are due to the elliptic form of the 10-MRs. Indeed, the effective pore widths calculated from the crystallographic data, by using an oxygen radius of 1.35 Å for these non-circular 10-MRs windows, are 7.28(3) Å for the main length and 3.14(2) Å for the small axis.

4. Conclusion

The germanosilicate IM-16 is a new member of the zeolites family prepared with the ionic liquid 3-ethyl-1-methyl-3*H*-imidazol-1-ium as a structure-directing agent. The structure of calcined IM-16 was solved from PXRD data in space group *Cmcm*. The framework topology is new and the crystallographic data have been transmitted to the Structure-Commission of the International Zeolite Association for a code assignment [11b]. IM-16 is stable after calcination but only under dry atmosphere. Further crystallographic studies (PXRD and solid state NMR) on as-synthesised IM-16 are in progress.

Acknowledgments

We thank the Centre National de la Recherche Scientifique and IFP for a Doctoral Grant to Y.L. (Agreement no. 50163400) and for support and the Ministère de la Recherche for a Doctoral Grant to M.D. (Agreement no. 28314). We acknowledge Claire Marichal and Séverinne Rigolet for assistance in performing solid-state NMR measurements.

Appendix A. Supplementary data

Supplementary data associated with this article can be found in the online version at doi:10.1016/j.jssc.2008.12.002.

(1), (2) and (3) Chemical analyses of as-synthesised IM-16; (4) CIF file of calcined IM-16. Further details of the crystal structure investigation can be also obtained from the Fachinformationszentrum Karlsruhe, 76344 Eggenstein-Leopold-shafen, Germany, (fax: +49 7247 808 666; e-mail: crystaldata@-fiz.karlsruhe.de) on quoting the depository number CSD-419952.

References

[1] J. Yu, in: J. Čejka, H. van Bekkum, A. Corma, F. Schüth (Eds.), Studies in Surface Science and Catalysis: Introduction to Zeolite Science and Practice, vol. 168, Elsevier, Amsterdam, The Netherlands, 2007, pp. 39–103 (Chapter 3 and references therein).
[2] [a] A.W. Burton, S.I. Zones, S. Elomari, Curr. Opinion Colloid Interface Sci. 10 (2005) 211;
[b] S.I. Zones, S.-J. Hwang, S. Elomari, I. Ogino, M.E. Davis, A.W. Burton, C. R. Chim. 8 (2005) 267;
[c] A.W. Burton, G.S. Lee, S.I. Zones, Micropor. Mesopor. Mater. 90 (2006) 129;
[d] J.L. Guth, H. Kessler, R. Wey, in: Y. Murakami, A. Iijima, J.W. Ward (Eds.), Studies in Surface Science and Catalysis: New Developments in Zeolite Science and Technology, vol. 28, Elsevier, Amsterdam, The Netherlands, 1986, p. 121;
[e] M. Camblor, L. Villaescusa, M. Diaz-Cabanas, Top. Catal. 9 (1999) 59;
[f] A. Corma, M.E. Davis, ChemPhysChem 5 (2004) 304;
[g] P. Caullet, J.-L. Paillaud, A. Simon-Masseron, M. Soulard, J. Patarin, C. R. Chim. 8 (2005) 245.
[3] E.M. Flanigen, R.L. Patton, U.S. Patent 4 073 865;
E.M. Flanigen, R.L. Patton, Chem. Abstr. 88 (1978) 138653.
[4] [a] D.M. Chapman, A.L. Rol, Zeolites 10 (1990) 730;
[b] M.J. Annen, M.E. Davis, J.B. Higgins, J.L. Schlenker, J. Chem. Soc. Chem. Commun. (1991) 1175;
[c] G. Giannetto, J. Papa, J. Perez, L. Garcia, R. Monque, Z. Gabelica, Zeolites 14 (1994) 549;
[d] S. Vortmann, B. Marler, H. Gies, P. Daniels, Micropor. Mater. 4 (1995) 111;
[e] T. Blasco, A. Corma, M.J. Diaz-Cabanas, F. Rey, J.A. Vidal-Moya, C.M. Zicovich-Wilson, J. Phys. Chem. B 106 (2002) 2634.
[5] Y. Lorgouilloux, J.-L. Paillaud, P. Caullet, N. Bats, Solid State Sci. 10 (2008) 12.
[6] H. Li, O.M. Yaghi, J. Am. Chem. Soc. 120 (1998) 10569.
[7] T. Conradsson, M.S. Dadachov, X.D. Zou, Micropor. Mesopor. Mater. 41 (2000) 183.
[8] Y. Mathieu, J.-L. Paillaud, P. Caullet, N. Bats, L. Rouleau, Micropor. Mesopor. Mater. 75 (2004) 13.
[9] J.-L. Paillaud, B. Harbuzaru, J. Patarin, N. Bats, Science 304 (2004) 990.
[10] [a] C. Cascales, E. Gutierrez-Puebla, M.A. Monge, C. Ruiz-Valero, Int. J. Inorg. Mater. 1 (1999) 181;
[b] C. Cascales, B. Gomez-Lor, E. Gutierrez-Puebla, M. Iglesias, M.A. Monge, C. Ruiz-Valero, N. Snejko, Chem. Mater. 14 (2002) 677;
[c] H. Li, M. Eddaoudi, O.M. Yaghi, Angew. Chem. Int. Ed. 38 (1999) 653.

[11] [a] M. O'Keeffe, O.M. Yaghi, Chem. Eur. J. 5 (1999) 2796
[b] Ch. Baerlocher, L.B. McCusker, D.H. Olson, Atlas of zeolite framework types, Sixth Revised Edition; Elsevier B.V., Amsterdam, The Netherlands, 2007, also available on the web at: 〈http://www.iza-structure.org/databases/〉.
[12] E.R. Cooper, C.D. Andrews, P.S. Wheatley, P.B. Webb, P. Wormald, R.E. Morris, Nature 430 (2004) 1012.
[13] E.R. Parnham, R.E. Morris, Acc. Chem. Res. 40 (2007) 1005.
[14] French patent, in deposition, demand no. FR07/05.315.
[15] A. Boultif, D. Louër, J. Appl. Crystallogr. 24 (1991) 987.
[16] STOE WinXPOW, version 1.06, 1999.
[17] [a] A. Altomare, M.C. Burla, G. Cascarano, C. Giacovazzo, A. Guagliardi, A.G.G. Moliterni, G.J. Polidori, Appl. Crystallogr. 28 (1995) 842;
[b] A. Altomare, G. Cascarano, C. Giacovazzo, A. Guagliardi, M.C. Burla, G.J. Polidori, M. Camalli, J. Appl. Crystallogr. 27 (1994) 435.
[18] [a] A.C. Larson, R.B. Von Dreele, General Structure Analysis System, Los Alamos National Laboratory Report LAUR 86-748, 2000;
[b] B.H. Toby, J. Appl. Crystallogr. 34 (1994) 210.
[19] Cerius^2 Modelling Environment, Release 4.2MS, Accelrys Inc., San Diego, 2002.
[20] S. Brunauer, P.H. Emmett, E. Teller, J. Am. Chem. Soc. 60 (1938) 309.
[21] M.D. Foster, M.M.J. Treacy, A database of hypothetical zeolite structures available on the web at: 〈http://www.hypotheticalzeolites.net〉.